

# Compact Circularly Polarized Cavity-Backed Slot Antenna

Evgeniy R. Gafarov, Alexey A. Erokhin, Roman O. Ryazantsev, Anton M. Aleksandrin

**Abstract** – This paper presents a theoretical study of a cavity-backed circularly polarized slot antenna, designed for applications requiring high-quality polarization characteristics across a wide angular range. The analysis covers radiation patterns, polarization properties, and impedance matching across the operating frequency range. The proposed antenna demonstrates advantages in terms of compact size, ease of fabrication, and achievable performance characteristics. The antenna design achieves a high average axial ratio of approximately 0.96 in angular region from  $-50^\circ$  to  $50^\circ$  with small antenna size  $0.4\lambda_0$ .

**Keywords** – Slot Antenna, Cavity-Backed, Circular Polarization, Axial Ratio, Radiation Pattern

## I. INTRODUCTION

Currently, designs for circularly polarized antennas for various satellite systems, including navigation, communication, telecommunications, and others [1, 2], are rapidly advancing due to improvements in manufacturing technologies. Antennas designed to receive signals with right-hand (RHCP) and/or left-hand circular polarization (LHCP) are often employed in transceiver systems [3] to provide polarization discrimination and enhance channel isolation. Circularly polarized antennas serve as standalone elements in receiving systems for navigation, positioning, and timing [4, 5], or they can be integrated into antenna arrays to increase gain [6] or to counteract intentional and unintentional interferences [7]. Implementing linearly polarized elements with sequential rotation in an antenna array [8] implies their use for directional antenna devices, as circular polarization generated this way typically operates within a narrow angular sector. To achieve circular polarization over a wide angular sector, it is necessary to excite two orthogonal modes directly within a single radiating element. Such an element can then function either independently or as part of an array, depending on the system requirements. It is important to emphasize requirements for wide-angle circular polarization performance now apply not only to terrestrial antenna systems (e.g., GNSS base station receivers) [9] but also to antennas on emerging low-altitude spacecraft in low Earth orbit (LEO) [10]. The low orbital altitude imposes stringent requirements in the form of

*Article history: Received August 13, 2025; Accepted September 09, 2025.*

Evgeniy R. Gafarov, Alexey A. Erokhin, Roman O. Ryazantsev, Anton M. Aleksandrin are with the Institute of Engineering Physics and Radio Electronics, Siberian Federal University, 79 Svobodny pr., 660041 Krasnoyarsk, Russia, E-mail: egafarov@sfu-kras.ru, aeroxhin@sfu-kras.ru, rryazantsev@sfu-kras.ru, aalexandrin@sfu-kras.ru

wide angular beamwidth and polarization performance. Thus, the investigation of manufacturable and compact circularly polarized antennas capable of operating over a wide angular range represents a relevant task for both onboard and terrestrial systems of various purposes.

These requirements are met by a cavity-backed slot antenna. Numerous cavity-backed antenna designs based on substrate integrated waveguide (SIW) technology [11] are known. Such antennas can achieve a wide-angle radiation pattern [12] or, on the contrary, a relatively small beam width when combined into antenna array [13]. Additionally, SIW antennas can be matched to the feeder in wide frequency range [14] or in dual band with frequency ratio up to 30 [15]. Moreover, a frequency-tunable SIW cavity-backed antenna is known [16]. Tuning of the reflection coefficient is achieved using a disk aperture-coupled to the radiating slot. Despite their advantages, SIW antennas have leakage, dielectric and ohmic losses.

To minimize losses, all-metal antennas are employed. For example, in papers [17, 18] the authors developed such antennas. Antenna from [17] is wideband, it operates in frequency range from 10 to 16 GHz and has high gain about 16 dBi. Antenna from [18] is frequency-tunable by metal pin. Length of the pin changes an inductance and as a result resonant frequency changes. However, these antenna designs allow operation only in linear polarization.

To excite a circularly polarized wave, two spatially orthogonal electric field vectors with a  $90^\circ$  phase shift are required. So, in [19] authors developed slot antennas with  $90^\circ$  crossed slots to ensure circular polarization. This construction allows tuning antenna characteristics similarly to [18]. Besides, it is possible to use slots with more complex shape. In [20] authors employ arc slots to achieve high axial ratio in wide angular sector, but its antenna operates in narrow frequency band, 3 dB axial ratio bandwidth is about 0.4%. Using a circular slot [21], it is possible to achieve 3 dB axial ratio bandwidth about 9.5% with wide angular sector. However, these constructions have large electrical length and width about  $0.7\lambda_0$ , where  $\lambda_0$  is center operating frequency.

Other types of antennas that form polarization characteristics over a wide angular sector are also known, such as, for example, low-profile single- or multi-layer printed antennas with high-impedance surfaces [22], Fabry-Perot resonator-based antennas with artificial magnetic conductor [23], helical antennas [24], and quadrifilar antennas [25]. The disadvantages of these antennas include their large longitudinal or transverse dimensions.

In this paper, we focused on compact ( $0.4\lambda_0$ ) all-metal antenna with ring slot to achieve high axial ratio in wide angular sector. We study the antenna elements to evaluate their characteristics.

## II. ANTENNA DESIGN

In this work, a low-profile cavity-backed slot antenna is investigated. The antenna was modeled using the Finite Element Method (FEM) in electromagnetic simulation software.

### A. Antenna assembly

The assembled antenna view is shown in Fig. 1(a). An interior view of the antenna cavity is presented in Fig. 1(b). The slot element ("slot" in Fig. 1(c)), etched into the ground plane, is located on the top side of the antenna.

To reduce the antenna's lateral size, the slot features a cogwheel shape. The antenna cavity ("cavity" in Fig. 1c) forms an electrically closed cylindrical volume filled with the Rohacell – a structural polymethacrylimide foam having parameters  $\epsilon_r = 1.05$ ,  $\tan\delta = 0.0002$ . The cavity is filled using two layers of Rohacell, each 4 mm thick. This configuration is used to create a suspended substrate for the balanced stripline forming the branchline coupler feed network. To ensure compactness and increase packing density, the branchline coupler striplines are implemented with multiple meanders.

The feed network is excited via the center conductor of a coaxial cable ("coax") at the geometric center of the antenna. The two outputs of the feed network are shorted to the cavity wall at points "1" and "2" on the cavity periphery, as shown in the top view of Fig. 1(c). The shorted feed outputs enable energy transfer to the slot radiating element ("slot"). Importantly, this feeding method is only valid for a balanced stripline where electric field concentration occurs both above and below the strip.

To ensure mechanical stability and flatness of the slot radiator ("slot"), the central part of the antenna's top ground plane is secured by four dielectric spacers. The spacer material is Teflon (PTFE) with  $\epsilon_r = 2.1$ ,  $\tan\delta = 0.0002$ . The top ground plane is fastened to the spacers using metric dielectric screws made of PTFE. The antenna height is  $H = \lambda_0 / 16$  (where  $\lambda_0$  is the free-space wavelength), and its diameter is  $D = 0.4\lambda_0$ .

The resonant frequency of the proposed antenna is determined primarily by the slot radiator length and secondarily by the cavity volume acting as a resonator [26]. The frequency at which the axial ratio reaches its maximum value (maximum circular polarization purity) is determined by the quadrature hybrid feed network [27].

### B. Cavity-backed Shaped Slot

An initial study of the compact slot radiator with a cavity was conducted to determine its resonant frequency. The following section examines an antenna excited by the two fundamental orthogonal modes in quadrature.

Fig. 2 depicts an antenna with a compact gear-shaped slot radiator, featuring a smaller diameter  $D_1 = 47.5$  mm and a bigger diameter  $D_2 = 57.5$  mm. The resonant cavity has an outer diameter  $D = 64$  mm, corresponding to  $0.4\lambda_0$ . The slot length is approximately  $1.5\lambda_0$ , and the slot width is  $S = 1$  mm.

The antenna excitation was implemented using two striplines rotated  $90^\circ$  relative to each other. The output

amplitudes are equal, with a phase shift of  $90^\circ$  to achieve sequential rotation excitation.

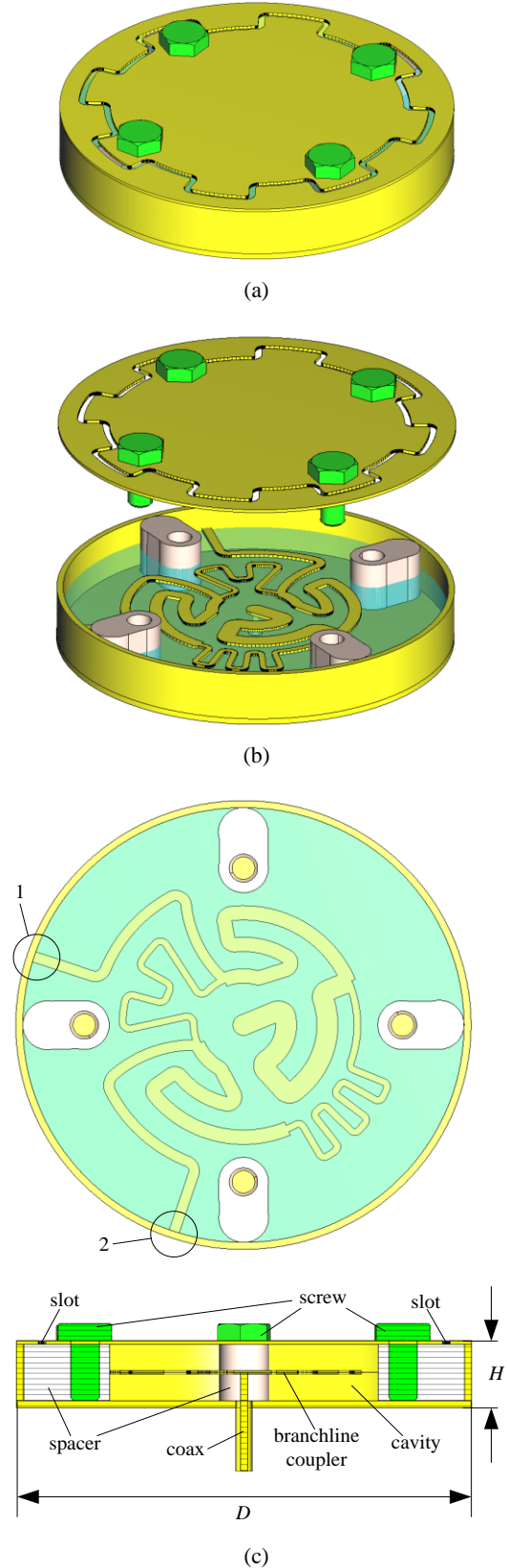


Fig. 1. Cavity-backed slot antenna: (a) assembled antenna, (b) view of antenna cavity, (c) top view of feed network and cutting plane of assembled antenna

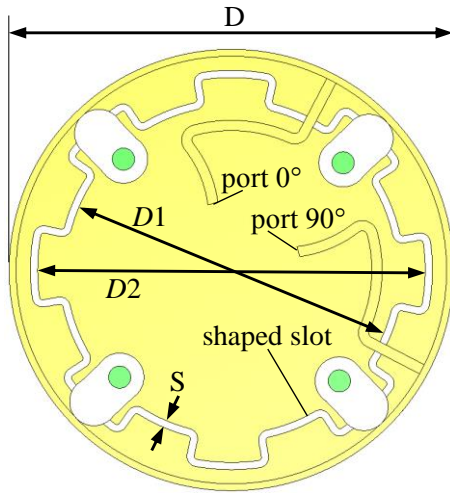


Fig. 2. The pinion gear shaped slot with stripline quadrature fed

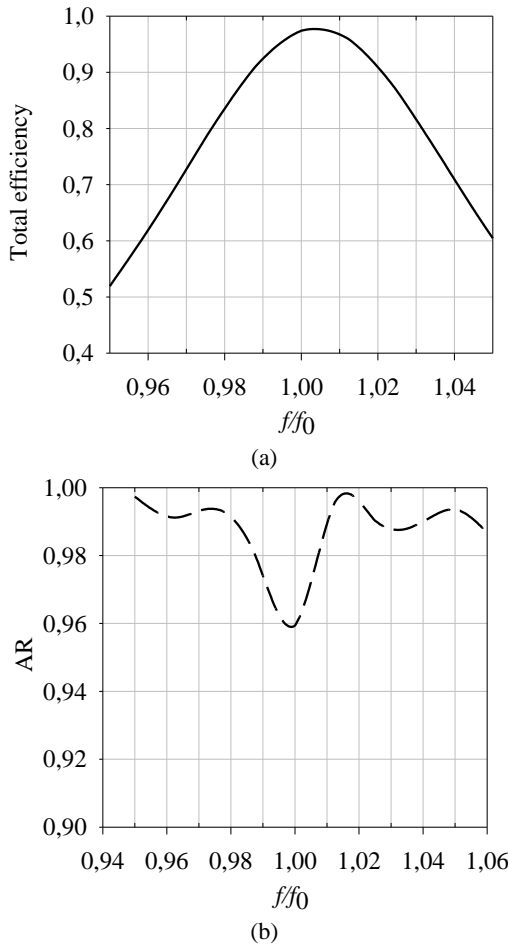


Fig. 3. (a) Frequency dependences of total efficiency, (b) average axial ratio at area  $\theta = [-50^\circ; 50^\circ]$

The total efficiency (including mismatch and dissipative losses) exceeds 0.9 within the frequency band  $f/f_0 = 0.99 - 1.02$  (Fig. 3(a)). The frequency dependence of the axial ratio (Fig. 3(b)) demonstrates that the antenna maintains favorable polarization characteristics outside its efficiency-based operational bandwidth. It should be noted that

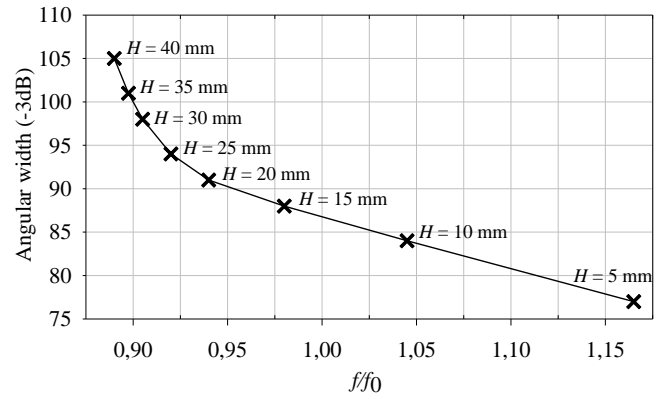


Fig. 4. Frequency dependence of angular width for different antenna cavity height ( $H$ )

axial ratio of the assembled antenna will also be determined by its feed network and the matching of the slot radiator, which is inherently narrowband for antennas of this type.

Next, a study was conducted to investigate the effect of the cavity height on the radiation pattern angular width of the slot antenna. Figure 4 shows the frequency dependence of the angular width (-3 dB) for cavity heights ( $H$ ) ranging from 5 mm to 40 mm in 5 mm steps.

The graph shows that as the height  $H$  increases, the angular width also increases. Initially, up to a height of  $H = 20$  mm, the characteristic grows linearly, after which the angular width sharply rises. This may be due to the fact that the current distributions on the conductor's surface are such that the cavity-backed antenna degenerates into an omnidirectional monopole-like antenna over a ground plane.

It should also be noted that the obtained variability in angular width with respect to  $H$ —ranging from  $77^\circ$  to  $105^\circ$  for the proposed compact antenna allows for selecting different configurations to address a wide range of applications, including both terrestrial and satellite systems for various purposes.

Next, we will examine the configuration of a compact feeding circuit for exciting the slot antenna in quadrature.

### C. Compact Feed Network

The key component in designing a circularly polarized antenna is the feeding circuit. A properly designed feeding circuit ensures high axial ratio within the specified operating frequency band. A two-point feeding scheme was proposed. Although feeding schemes with three or more points can provide better polarization characteristics, they require more space and are unsuitable for the proposed antenna design.

For a compact antenna implementation, even a conventional quadrature hybrid coupler is not suitable, as the dimensions of its topology may exceed the inner diameter of the slot radiator ( $D1$  in Fig. 2, see Fig. 5 on the left). In this case, spontaneous excitation of the slot radiator may occur, leading to degraded polarization characteristics.

To achieve a compact feeding solution, a folded quadrature hybrid coupler based on a stripline is proposed, with a reference characteristic impedance of  $Z_0 = 110 \Omega$ . The physical layout is shown in the figure 5.

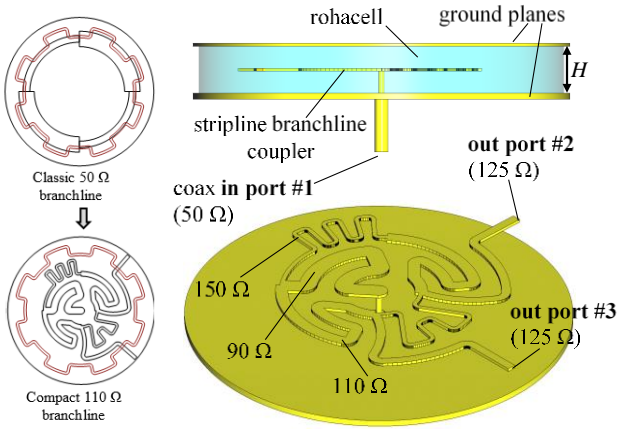
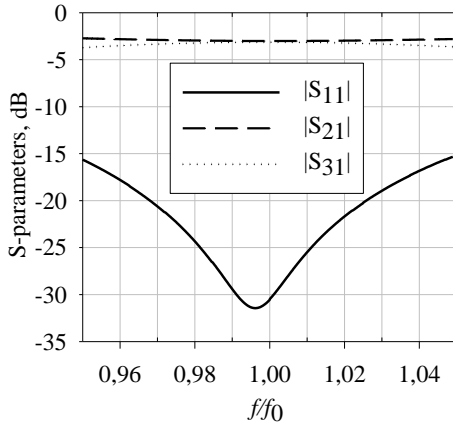
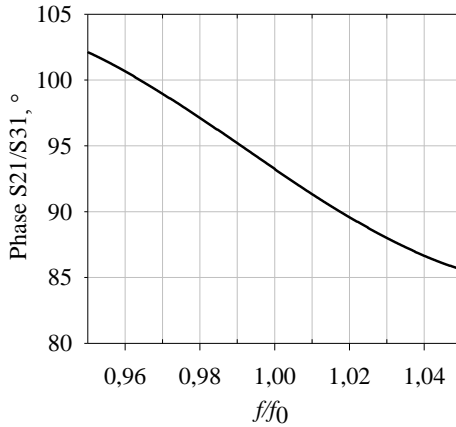


Fig. 5. The stripline feed network – compact branchline coupler with reference characteristic impedance  $Z_0 = 110 \Omega$



(a)



(b)

Fig. 6. (a) Frequency dependences of magnitude of  $S$ -parameters, (b) phase of  $S$ -parameters

The design is based on a stripline feeding circuit with a height of  $H = 8$  mm, since unlike microstrip lines, the electric field propagates symmetrically between the upper and lower ground planes, eliminating the need to route the feed cable directly to the antenna excitation point. A characteristic impedance of  $Z_0 = 110 \Omega$  allowed for a reduction in the width of the feeding circuit conductors, freeing up space for implementing bends in the quadrature hybrid. However, a

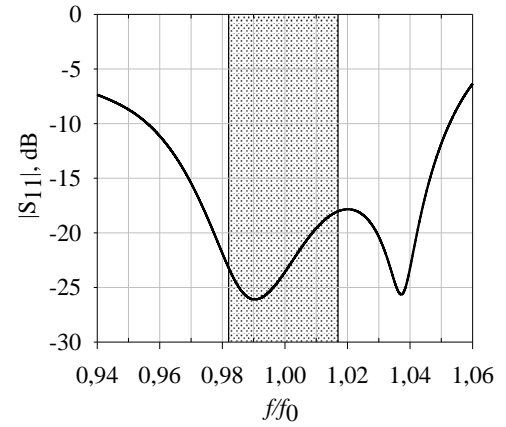
$95 \Omega$  stripline transformer had to be added at the input to ensure matching. The input impedance of the feeding circuit is  $50 \Omega$ , while the high-impedance sections have a characteristic impedance of  $Z_1 = \sqrt{2} \cdot Z_0 \approx 150 \Omega$ . The output ports of the feeding circuit are designed for  $125 \Omega$  to ensure optimal matching between the slot radiator and the feedline.

Below, Figs. 6(a) and 6(b) present the amplitude and phase characteristics of the compact quadrature hybrid-based feeding circuit.

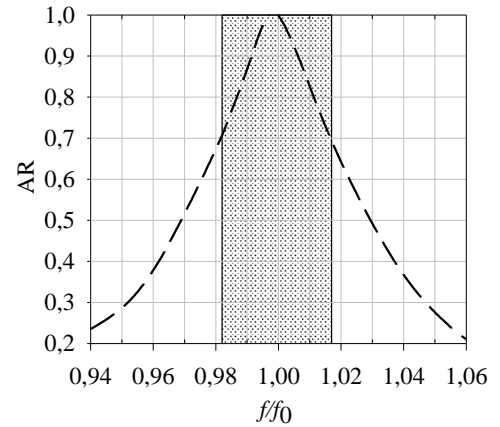
The compact feeding circuit implementation features equal power division between two outputs with approximately  $90^\circ$  phase difference between them, similar to a full-size feeding circuit (classic  $50 \Omega$  branchline coupler).

### III. SIMULATED RESULTS AND DISCUSSION

To analyze the cavity-backed slot antenna assembly, its impedance matching, radiation pattern, and polarization properties were calculated.



(a)



(b)

Fig. 7. (a) Frequency dependences of the  $|S_{11}|$  magnitude, (b) the axial ratio at zenith

Figure 7(a) shows the reflection coefficient  $|S_{11}|$  versus normalized frequency ( $f/f_0$ ), where  $f_0$  is the antenna's central frequency. The antenna exhibits a low  $|S_{11}|$ , with a  $-10$  dB bandwidth of approximately 10% and a  $-15$  dB bandwidth of about 8%. However, the bandwidth for an axial ratio ( $AR$ )  $> 0.7$  is approximately 4%, which is indicated by the shaded region in Fig. 7(b). This bandwidth is defined as the operational bandwidth.



Fig. 7(b) shows that the axial ratio approaches its maximum value ( $AR \approx 1$ , indicating optimal circular polarization) only near normalized frequency  $f/f_0 \approx 1$ . This can be attributed to the resonant nature of the slot radiator, despite the branchline coupler feed network providing equal-amplitude quadrature excitation over a  $\sim 10\%$  bandwidth [27].

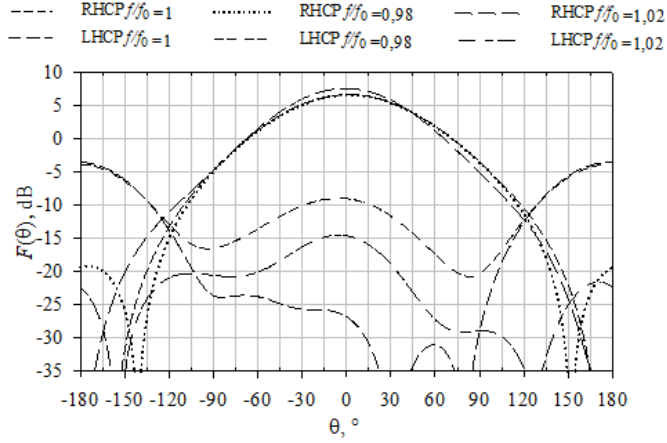


Fig. 8. Radiation patterns for left and right circular polarization

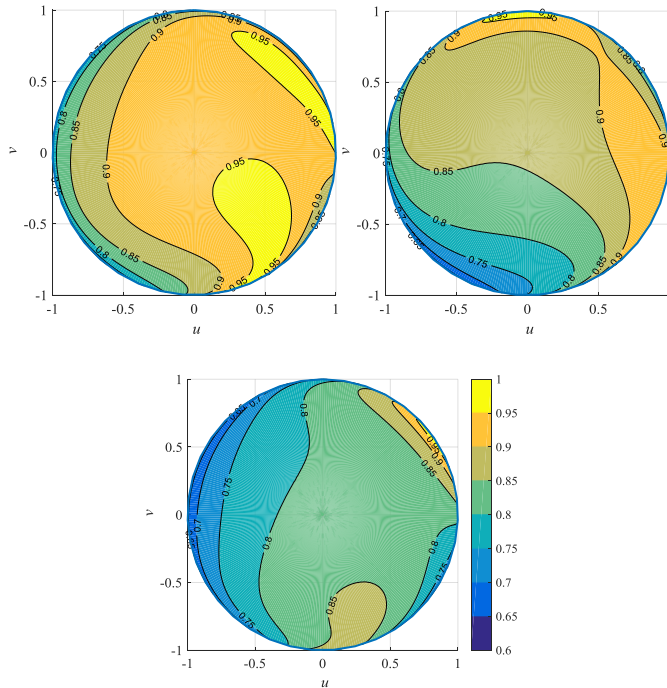


Fig. 9. (a) Axial ratio at  $f/f_0 = 1$ , (b)  $f/f_0 = 0.98$ , (c)  $f/f_0 = 1.02$

Fig. 8 presents the radiation patterns for right-hand (RHCP) and left-hand circular polarization (LHCP) at the center frequency ( $f/f_0 = 1$ ), at lower band-edge frequency ( $f/f_0 = 0.98$ ) and at higher band-edge frequency ( $f/f_0 = 1.02$ ). The choice of radiation pattern cut plane (Fig. 8) is non-critical, as the antenna's symmetric design results in near-zero azimuthal pattern variation.

The antenna gain is 6.5 dBi, with a half-power angular width of  $90^\circ$ . Furthermore, Fig. 8 indicates good polarization discrimination. The axial ratio for RHCP (RHCP/LHCP ratio in Fig. 8) is better than 0.8 over  $\theta = [-90^\circ; 90^\circ]$  at the center frequency and remains above 0.65 at the frequency band edge.

These high AR values across a wide angular sector stem from the excitation of orthogonal electric field components in the antenna's top plane [28].

Fig. 9 shows patterns of the axial ratio in normalized u/v coordinates. The elevation angle in Fig. 9 varies from  $-90^\circ$  to  $90^\circ$ . High values of the axial ratio are observed both for the zenith direction and for the periphery, up to the edge of the spatial hemisphere. It should be emphasized that the wide-angle AR performance is enabled by the antenna's air-gap cavity design. Comparable low-profile antennas, such as conventional patch antennas [29] also employing an air substrate, achieve high AR values over only half the angular sector due to electric field confinement between the patch and ground plane.

#### IV. CONCLUSION

Slot antennas backed by a resonant cavity can provide circular polarization over a wide angular range ( $\pm 60^\circ$  or more). This cavity enhances polarization stability by shielding parasitic radiation and ensuring more uniform current distribution. This study has investigated a compact low-profile antenna with a diameter of  $0.4\lambda_0$ , providing high axial ratio (high circular polarization purity) across a wide angular sector  $[-90^\circ; 90^\circ]$ . Compared to modern antennas of other types that form similar polarization characteristics, the proposed antenna features small transverse dimensions and can be used in applications where implementation compactness is important, including in small-sized antenna arrays. A limitation of the proposed antenna is its relatively narrow operating frequency band, limited by the slot radiator, which may not always be suitable for use in certain broadband systems.

Thus, the antenna features a simple design with a quadrature feed circuit for circular polarization excitation and can be manufactured using modern techniques, including metal additive manufacturing (3D printing).

#### ACKNOWLEDGEMENT

This work was supported by the Russian Science Foundation under grant no. 25-19-20106, <https://rscf.ru/project/25-19-20106/>, grant of Krasnoyarsk Regional Fund of Science.

#### REFERENCES

- [1] T. Hadas, K. Kazmierski, I. Kudłacik, G. Marut and S. Madraszek, "Galileo High Accuracy Service in Real-Time PNT, Geoscience and Monitoring Applications," *IEEE Geoscience and Remote Sensing Letters*, vol. 21, pp. 1-5, 2024, DOI: 10.1109/LGRS.2024.3354293
- [2] E. Boni, G. Giannetti, S. Maddio and G. Pelosi, "A Circular Polarized Antenna for GPS and Iridium Applications," *2023 IEEE International Symposium on Antennas and Propagation and USNC-URSI Radio Science Meeting (USNC-URSI)*, Portland, OR, USA, 2023, pp. 195-196, DOI: 10.1109/USNC-URSI52151.2023.10237948
- [3] W. J. Krzysztofik, "Coplanar-Square-Patch Antenna for Iridium Satellite Reception," *2006 First European Conference on Antennas and Propagation*, Nice, France, 2006, pp. 1-4, DOI: 10.1109/EUCAP.2006.4584566

- [4] A. Leick, L. Rapoport, and D. Tatarnikov, *GPS Satellite Surveying*, Wiley, 2015, ISBN: 9781118675571
- [5] P. J. Teunissen and O. Montenbruck, *Springer Handbook of Global Navigation Satellite Systems*, Springer International Publishing, 2017, ISBN: 9783030731724
- [6] E. R. Gafarov, A. A. Erokhin, Y. P. Salomatov, Y. A. Strigova, A. M. Aleksandrin and A. N. Vereshagin, "The Circular Polarized Antenna Array for Cube Satellites", *2023 Radiation and Scattering of Electromagnetic Waves (RSEMW)*, Divnomorskoe, Russian Federation, 2023, pp. 388-391, DOI: 10.1109/RSEMW58451.2023.10202038
- [7] I. T. McMichael, E. Lundberg, D. Hanna and S. Best, "Horizon Nulling Helix Antennas for GPS Timing", *2017 IEEE International Symposium on Antennas and Propagation & USNC/URSI National Radio Science Meeting*, San Diego, CA, USA, 2017, pp. 2495-2495, DOI: 10.1109/APUSNCURSINRSM.2017.8073290
- [8] G. Tian, L. Lizhang and G. Li, "A Broadband Circularly Polarized Antenna Array Based on Sequential Rotation Feeding", *2024 IEEE International Workshop on Radio Frequency and Antenna Technologies (iWRF&AT)*, Shenzhen, China, 2024, pp. 395-397, DOI: 10.1109/iWRFAT61200.2024.10594319
- [9] G. Rahul and D. Srinivasan, "11m L&S Band Ground Station Antenna for Indian Navigation Satellite Signal Monitoring", *2021 International Conference on Intelligent Technologies (CONIT)*, Hubli, India, 2021, pp. 1-4, DOI: 10.1109/CONIT51480.2021.9498271
- [10] Z. P. Zhong, X. Zhang, J. J. Liang, C. Z. Han, M. L. Fan and G.-L. Huang, "A Compact Dual-Band Circularly Polarized Antenna with Wide Axial-Ratio Beamwidth for Vehicle GPS Satellite Navigation Application", *IEEE Transactions on Vehicular Technology*, vol. 68, no. 9, pp. 8683-8692, Sept. 2019, DOI: 10.1109/TVT.2019.2920520
- [11] E. Aparna, G. Ram and G. A. Kumar, "Review on Substrate Integrated Waveguide Cavity Backed Slot Antennas," *IEEE Access*, vol. 10, pp. 133504-133525, 2022, DOI: 10.1109/ACCESS.2022.3231984
- [12] A. Kumar, "Substrate Integrated Waveguide Cavity-Backed Slot Antenna with Low Cross-Polarization over the Full Bandwidth", *Microwave and Optical Technology Letters*, vol. 66, no. 1, Jan. 2024, DOI: 10.1002/mop.34019
- [13] W. Zhang, K. Han, Z. Jiang and Z. Yan, "Bandwidth-Enhanced Design of Compact High-Order-Mode Cavity-Backed Slot Antenna", *IEEE Antennas and Wireless Propagation Letters*, vol. 23, no. 12, pp. 4338-4342, Dec. 2024, DOI: 10.1109/LAWP.2024.3445628
- [14] K. Sultan and A. Abbosh, "On-Body Cavity-Backed Slot Antenna with Pattern and Polarization Diversity for Medical Imaging", *IEEE Transactions on Antennas and Propagation*, vol. 72, no. 11, pp. 8239-8250, Nov. 2024, DOI: 10.1109/TAP.2024.3453394
- [15] Q. J. Deng, Y. M. Pan, X. Y. Liu and K. W. Leung, "A Singly-Fed Dual-Band Aperture-Sharing SIW Cavity-Backed Slot Antenna with Large Frequency Ratio", *IEEE Transactions on Antennas and Propagation*, vol. 71, no. 2, pp. 1971-1976, Feb. 2023, DOI: 10.1109/TAP.2022.3232208
- [16] R. Agasti, C. G. Blosser, J. E. Ruyle and H. H. Sigmarsson, "Tunable SIW-Based Evanescent-Mode Cavity-Backed Slot Antenna with Contactless Tuning", *IEEE Access*, vol. 11, pp. 42670-42678, 2023, DOI: 10.1109/ACCESS.2023.3265571
- [17] Y. Asci, "Wideband and Stable-Gain Cavity-Backed Slot Antenna With Inner Cavity Walls and Baffle for X- and Ku-Band Applications", *IEEE Transactions on Antennas and Propagation*, vol. 71, no. 4, pp. 3689-3694, April 2023, DOI: 10.1109/TAP.2023.3239168
- [18] R. -S. Chen, L. Zhu, S. -W. Wong, X. -Z. Yu, Y. Li and W. He, "Novel Reconfigurable Full-Metal Cavity-Backed Slot Antennas Using Movable Metal Posts", *IEEE Transactions on Antennas and Propagation*, vol. 69, no. 10, pp. 6154-6164, Oct. 2021, DOI: 10.1109/TAP.2021.3069584
- [19] R. S. Chen, X. D. Li, H. L. Liu, G. L. Huang, S. W. Wong, M.K.T. Al-Nuaimi, "Reconfigurable Full-Metal Circularly-Polarized Cavity-Backed Slot Antenna and Array with Frequency and Polarization Agility", *IEEE Transactions on Circuits and Systems II: Express Briefs*, vol. 70, no. 2, pp. 531-535, Feb. 2023, DOI: 10.1109/TCSII.2022.3215951
- [20] Y. Xu, Z. Wang and Y. Dong, "Circularly Polarized Slot Antennas with Dual-Mode Elliptic Cavity", *IEEE Antennas and Wireless Propagation Letters*, vol. 19, no. 4, pp. 715-719, April 2020, DOI: 10.1109/LAWP.2020.2978343
- [21] R. S. Chen, L. Zhu, S. W. Wong, J. Y. Lin, Y. Li, L. Zhang, "S-Band Full-Metal Circularly Polarized Cavity-Backed Slot Antenna with Wide Bandwidth and Wide Beamwidth", *IEEE Transactions on Antennas and Propagation*, vol. 69, no. 9, pp. 5963-5968, Sept. 2021, DOI: 10.1109/TAP.2021.3061116
- [22] E. R. Gafarov and Y. P. Salomatov, "Hexagonal FSS for GLONASS/GPS Antenna with Improved Axial Ratio", *2011 International Siberian Conference on Control and Communications (SIBCON)*, Krasnoyarsk, Russia, 2011, pp. 159-161, DOI: 10.1109/SIBCON.2011.6072620
- [23] R. Fakhte and I. Aryanian, "Compact Fabry-Perot Antenna with Wide 3 dB Axial Ratio Bandwidth Based on FSS and AMC Structures", *IEEE Antennas and Wireless Propagation Letters*, vol. 19, no. 8, pp. 1326-1330, Aug. 2020, DOI: 10.1109/LAWP.2020.2999745
- [24] A. A. Erokhin, E. R. Gafarov, Y. P. Salomatov, S. V. Polenga, A. M. Aleksandrin and R. O. Ryazantsev, "Horizon Nulling Backfire Helix Antenna for Interference-Resistant GNSS Applications", *IEEE 25th International Conference of Young Professionals in Electron Devices and Materials (EDM)*, Altai, Russian Federation, 2024, pp. 380-383, DOI: 10.1109/EDM61683.2024.10615086
- [25] D. Zhao, G. Liu, G. Liu and C. Gu, "A Compact Dual-Band Assembled Quadrifilar Helix Antenna for LEO Satellite Communications", *International Conference on Microwave and Millimeter Wave Technology (ICMMT)*, Qingdao, China, 2023, pp. 1-3, DOI: 10.1109/ICMMT58241.2023.10276510
- [26] X.-X. Qin, N. -W. Liu and J. Chen, "Wideband Cavity-Backed Slot Antenna Based on Multi-Resonant Modes", *2021 IEEE International Workshop on Electromagnetics: Applications and Student Innovation Competition (iWEM)*, Guangzhou, China, 2021, pp. 1-3, DOI: 10.1109/iWEM53379.2021.9790631
- [27] V. Sinchangreed, M. Uthansakul and P. Uthansakul, "Design of Tri-Band Quadrature Hybrid Coupler for WiMAX Applications", *2011 International Symposium on Intelligent Signal Processing and Communications Systems (ISPACS)*, Chiang Mai, Thailand, 2011, pp. 1-4, DOI: 10.1109/ISPACS.2011.6146090
- [28] Y. Xu, Z. Wang and Y. Dong, "Circularly Polarized Slot Antennas with Dual-Mode Elliptic Cavity", *IEEE Antennas and Wireless Propagation Letters*, vol. 19, no. 4, pp. 715-719, April 2020, DOI: 10.1109/LAWP.2020.2978343
- [29] E. R. Gafarov, A. A. Erokhin, A. V. Stankovsky and Y. P. Salomatov, "Multiband Three-Layer GNSS Microstrip Antenna", *2019 International Siberian Conference on Control and Communications (SIBCON)*, Tomsk, Russia, 2019, pp. 1-4, DOI: 10.1109/SIBCON.2019.8729623